



Evidence for glacial deposits during the Little Ice Age in Ny-Alesund, western Spitsbergen

ZHONGKANG YANG^{1,2}, WENQING YANG¹, LINXI YUAN¹, YUHONG WANG¹
and LIGUANG SUN^{1,*}

¹Anhui Province Key Laboratory of Polar Environment and Global Change, School of Earth and Space Sciences, University of Science and Technology of China, Hefei 230 026, China.

²College of Resources and Environment, Key Laboratory of Agricultural Environment, Shandong Agricultural University, Tai'an 271 000, China.

*Corresponding author. e-mail: slg@ustc.edu.cn

MS received 11 September 2018; revised 20 July 2019; accepted 23 July 2019

The glaciers act as an important proxy of climate changes; however, little is known about the glacial activities in Ny-Alesund during the Little Ice Age (LIA). In the present study, we studied a 118-cm-high palaeo-notch sediment profile YN in Ny-Alesund which is divided into three units: upper unit (0–10 cm), middle unit (10–70 cm) and lower unit (70–118 cm). The middle unit contains many gravels and lacks regular lamination, and most of the gravels have striations and extrusion pits on the surface. The middle unit has the grain size characteristics and origin of organic matter distinct from other units, and it is likely the glacial till. The LIA in Svalbard took place between 1500 and 1900 AD, the middle unit is deposited between 2219 yr BP and AD 1900, and thus the middle unit is most likely caused by glacier advance during the LIA. Glaciers during the LIA likely overran the sampling site, removed part of the pre-existing sediments, and contributed to the formation of diamicton in the middle unit. This study provides evidence for glacial deposits during the LIA in Ny-Alesund and improves our understanding about historical glacier dynamics and ice-sheet margins during the LIA in western Spitsbergen.

Keywords. More extensive glaciers; Little Ice Age; Younger Dryas; western Spitsbergen.

1. Introduction

The Svalbard was totally covered by the Late Weichselian Barents ice sheet during the Last Glacial Maximum, and the Svalbard-Barents Sea Ice Sheet collapsed between 15 and 12 ka BP, causing widespread retreat of the northwestern margin from the shelf area into the modern coastline of the Svalbard archipelago (Hormes *et al.* 2013; Hughes *et al.* 2016). The deglaciation occurred from major troughs

and fjords to inter-trough and terrestrial realms, and the deglaciation time at different locations on Svalbard varied (Hormes *et al.* 2013; Landvik *et al.* 2014). Henriksen *et al.* (2014) studied the radiocarbon ages of marine sediments from the Kongsfjorden area, and reported the deglaciation of the fjord between 16.6 and 14.4 ka BP. Svendsen and Mangerud (1997) reported that there were no glaciers in the catchment of Linnevatnet, western Spitsbergen during the early and mid-Holocene, and glaciers advanced at

3.0, 2.4–2.5, 1.4–1.5 ka, and in the Little Ice Age (LIA) with the maximum extent of advances, consistent with the detailed review results of Holocene glacier fluctuations (Solomina *et al.* 2015, 2016). Glacier, as a sensitive climate proxy, has been regarded as an excellent indicator of climate change (Oerlemans 2005), and most Holocene terrestrial paleoclimate studies on Svalbard have focused on glaciers (Reusche *et al.* 2014; Røthe *et al.* 2015; van der Bilt *et al.* 2015; Gregory *et al.* 2017).

The glaciers in Svalbard during the Holocene are still poorly understood due to scarceness of well-constrained (pre-LIA) chronologies for glacial events (Farnsworth *et al.* 2017) and damage to the terrestrial evidence of earlier glacier moraine during the LIA (Bakke and Paasche 2011). Many glacier activities have been reconstructed for the Neoglacial period, culminating in the LIA (Solomina *et al.* 2015, 2016; Arppe *et al.* 2017; Grabiec *et al.* 2018). According to the reconstructed equilibrium-line-altitude (ELA) for Karlbreen, the LIA period on Svalbard spans intervals from 450 yr BP to the 20th century (Røthe *et al.* 2015). In western Spitsbergen, the increased glacier expansions started at the mid-14th century (Solomina *et al.* 2016). Continuous sequence of glacial varves in Kongressvatnet were observed from AD 1350 to 1880 (Guilizzoni *et al.* 2006). Szczuciński *et al.* (2009) reported the increased activity of Nordenskiöldbreen glacier between CE 1520 and 1900. Glacier Karlbreen reached its Holocene maximum extent at CE 1725 and 1815 (Røthe *et al.* 2015). However, studies about the glacier activities and glacial deposits during the LIA in Ny-Alesund are rare. Mangerud and Landvik (2007) demonstrated that the glaciers during the Younger Dryas (YD) in western Spitsbergen are less extensive than those during the LIA; however, the evidence could only be found at a few sites (Svendsen and Mangerud 1997; Salvigsen and Høgvard 2006; Mangerud and Landvik 2007) and are not conclusive.

In this study, we identified a glacial till deposit of the LIA in a palaeo-notch sediment for the first time in Ny-Alesund. Considering that the extent of glaciers during the LIA in Ny-Alesund has rarely been reported, the results of this study may shed light on the glacial activities during the LIA in Ny-Alesund.

2. Study area

Svalbard includes all the islands situated between 74°–81°N, and 10°–35°E, and its total surface area is approximately 63,000 km². The

largest island of Svalbard is Spitsbergen, with an area of 39,000 km². To the east of Spitsbergen, there are Nordaustlandet (14,500 km²), Edgeoya (5000 km²), Barentsoya (1300 km²) and numerous smaller islands (figure 1). Svalbard is located near the interface of warm and cold waters between the Arctic and the world's oceans, which make its climate considerably different from anywhere else in the Arctic (van der Bilt *et al.* 2015; Gregory *et al.* 2017).

The vast ice sheets in Svalbard reduced after the Last Glacial Maximum; but there is still sufficient ice left to cover large parts of the landscape, and about 60% of the land area of Svalbard is covered by glaciers. During the LIA maximum, the glacier area of Svalbard was 38,871 km², and after the LIA, the total ice area loss was 13.1% (Martín-Moreno *et al.* 2017). The glaciers are unevenly distributed on the archipelago; they are especially extensive in the north-east, and the ice-free areas are mainly concentrated in the western part of the island.

Ny-Alesund (78°55'N, 11°56'E) is located on the western coast of Spitsbergen (figure 1). In the Ny-Alesund area, the bedrock along the gentle coastal plateau is covered by glacial deposits and fluvial deposits (supplementary figure S1), and it mainly consists of a Middle Carboniferous–Early Triassic sedimentary sequence (Miccadei *et al.* 2016). The Ny-Alesund area is dominated by glacial and slope landforms on the SW mountainous area and in the main valleys, and characterized by a scattered cover of continental deposits (Miccadei *et al.* 2016). The terrestrial glaciers and valley glaciers retreated from the main valleys since the LIA and are now preserved in the mountain valleys (Hormes *et al.* 2013; Miccadei *et al.* 2016). The coast is characterized by gravel beaches on the NW side of Ny-Alesund, and anthropogenic landforms and deposits are also widespread and related to the intense coal mining (Miccadei *et al.* 2016). According to the meteorological station in Ny-Alesund (1979–2014) (Osuch and Wawrzyniak 2017), the mean annual temperature is −4.4°C. The coldest month is February, with an average of −12.4°C, and the warmest July, with 5.3°C. The average annual precipitation is 376 mm and the highest monthly precipitation is 51 mm in September. Most precipitation is related to cyclonic systems and occurs in winter and autumn months.

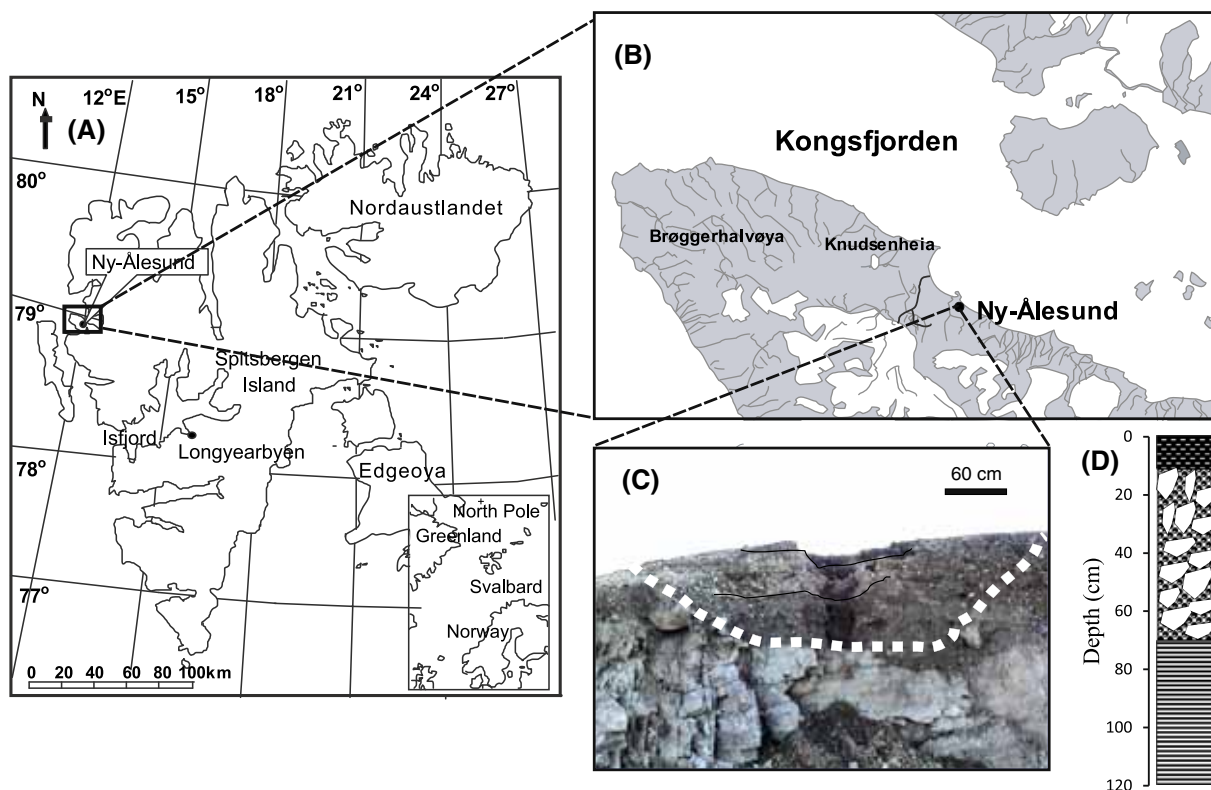


Figure 1. Map of studied area and sampling site. (A) location of Svalbard Islands, (B) location of Ny-Alesund, (C) field photograph of the palaeo-notch sediment profile, (D) lithology of the sediment profile YN.

3. Materials and methods

3.1 Sample collection

A rocky cliff occurs between the airport area and Ny-Alesund, where there is marine caves (Miccadei *et al.* 2016). In the field, we collected a 118-cm-high and well-preserved sediment profile named YN (78°55.6'N, 11°56.4'E) from the first terrace of Ny-Ålesund, Svalbard (figure 1). The sampling site is about 3 m away from the ocean and 3.5 m above sea level. This marine cave has been identified as a palaeo-notch (Yuan *et al.* 2010, 2011), though the cap of this notch does not exist now (figure 1); it is similar to the palaeo-notches discovered in Antarctic (Sun *et al.* 2005) and Arctic (Yang *et al.* 2018). This palaeo-notch opens towards the sea and has a smooth bottom of limestone. This palaeo-notch was formed by the erosion of ocean wave, and then became exposed and started to receive deposit after terrace uplift from the rapid isostatic rebound around 11000 yr BP (Sessford *et al.* 2015) or due to sea level decrease (Forman *et al.* 1987).

Based on colour and lithological characteristics, the sediment profile is divided into three units. The upper unit (0–10 cm) is a gray-black clay layer; its

colour is darker than the other units and this unit also contains some gravel with diameters varying from 1 mm to 1 cm. This unit was sectioned at 2 cm intervals and labeled as YN-1–YN-5. The middle unit (10–70 cm) is a brown gravel layer composed of clay-sandy matrix and gravels. This unit is poorly sorted and the lithology is notably distinct from other units. The middle unit contains many subangular and poorly oriented gravels with diameter varying from 3 mm to 5 cm, and ice scrapes could be observed on some of the gravels. The middle unit was sectioned at 10 cm intervals and labeled as YN-6–YN-11. The lower unit (70–118 cm) is a brown clay layer with shell remains and was sectioned at 2 cm intervals and labeled as YN-12–YN-35. In this study, we focus on the sedimentary anomaly of the middle unit. All the subsamples were frozen and brought back to laboratory for analysis.

3.2 Age dating

The chronology of sediment profile YN was established by both ^{210}Pb dating and AMS ^{14}C dating. For ^{210}Pb analysis, the top six consecutive sediment samples were processed to measure the

activity of the excess ^{210}Pb . The analytical instrument is a low background and high purity Germanium (HPGe) Gamma Ray Spectrograph (GWL-DSPEC-PLUS) (AMETEK Company, USA). The oldest sediments determined by excess ^{210}Pb was located between the boundary of the upper and middle units, corresponding to around 1900 AD (supplementary figure S2). The chronology of the lower unit has been reported in our previous study (Yang *et al.* 2019) and this unit spans from 2219 to 9400 yr BP.

3.3 Elemental and isotopic analysis

We performed total organic carbon (TOC), total nitrogen (TN) and carbon isotopic analysis on 11 subsamples from the upper unit and the middle unit (supplementary table S1). Each sample was air-dried in a clean laboratory and homogenized with a mortar and pestle, and then sieved through a 200-mesh sieve. For analysis of TOC and TN, about 0.1–0.5 g of each powder sample was precisely weighted to measure TOC content by chemical volumetric method with a duplication error <0.05% (Ruiz-Fernández *et al.* 2003; Yuan *et al.* 2010). TN content was determined by Kjeldahl digestion method with an error <0.005% (Yuan *et al.* 2010). For carbon isotopic analysis, about 3–4 mg of powder sample was mixed with CuO powder and then placed in a quartz combustion tube together with pre-roasted CuO and Cu wire and a few pieces of thin silver ribbon. After evacuation and sealing under vacuum, the tubes were heated in an induction furnace at 875°C for 20 min. After cooling the tubes at room temperature, the resulting CO₂ gas was dehydrated, purified, and then separated in a high-vacuum gas transfer system. Isotope measurements were made on a Finnigan-MAT 251 mass spectrometer. The reproducibility of standard materials is within ±0.05%. The analysis was performed at Institute of Soil Science, Chinese Academy of Sciences.

The TOC and TN contents, and carbon isotopic compositions from the lower unit, four kinds of common tundra plants and local coal samples in Ny-Alesund were reported in our previous studies (Yuan *et al.* 2010).

3.4 Grain size analysis

First, 0.5 g of fully dispersed dry sample (>2 mm gravels are removed) was taken, 10 ml of H₂O₂ solution (10%) was added, and the mixture was

heated to 100°C for 30 minutes to remove organic matter. Then 10 ml of HCl solution (10%) was added to remove carbonate and shell fragments. Finally, all the samples were fully dispersed by adding 10 ml (NaPO₃)₆ (10%) and treated by ultrasonic for 15 minutes before measurement. The grain size was analyzed using the LS230 laser diffraction particle size analyzer (Beckman Coulter, Inc.).

4. Results and discussion

4.1 Analysis of visual morphology

The middle unit of the sediment profile YN contains many unevenly distributed gravels of varying sizes with the diameter from 3 mm to ~5 cm. This unit has three lithological characteristics distinct from the upper and lower units: (1) regular laminations are non-existent, and both sorting and psepchicity are poor; (2) the gravels are angular or sub-angular, and the size varies greatly; (3) most of the gravels have striations and extrusion pits on their surface (figure 2).

The morphological characteristics of these gravels indicate that the middle unit is likely formed by glaciers. Striations on stones have often been used as glacial criteria (Chen *et al.* 2014; Svendsen *et al.* 2015; Alonso-Muruaga *et al.* 2018; Assine *et al.* 2018; McClenaghan *et al.* 2018; Mottin *et al.* 2018; Swift *et al.* 2018). Under the proper conditions, existence of striations can be one of the most important criteria for glaciation, though absence does not necessarily oppose a glacial origin. During the process of glacier advance, the sliding of glacier ice over soft beds could generate a series of erosional and depositional processes (Evans *et al.* 2006). The gravels abraded by glacial erosion and grinding have certain characteristics, which can be well preserved and used to infer gravels' transport history and sedimentary environment. In addition, stones impacted by glacier activity are sharply angular (Sovetov 2015; Ali *et al.* 2017). The morphological characteristics of the stones in sediment profile YN (middle unit) are consistent with those impacted by glaciers, and thus the middle unit is likely related to glacier advance.

4.2 Grain size characteristics

The grain size distribution characteristics have widely been used to the study of sedimentary processes (Sun *et al.* 2005), and the grain size

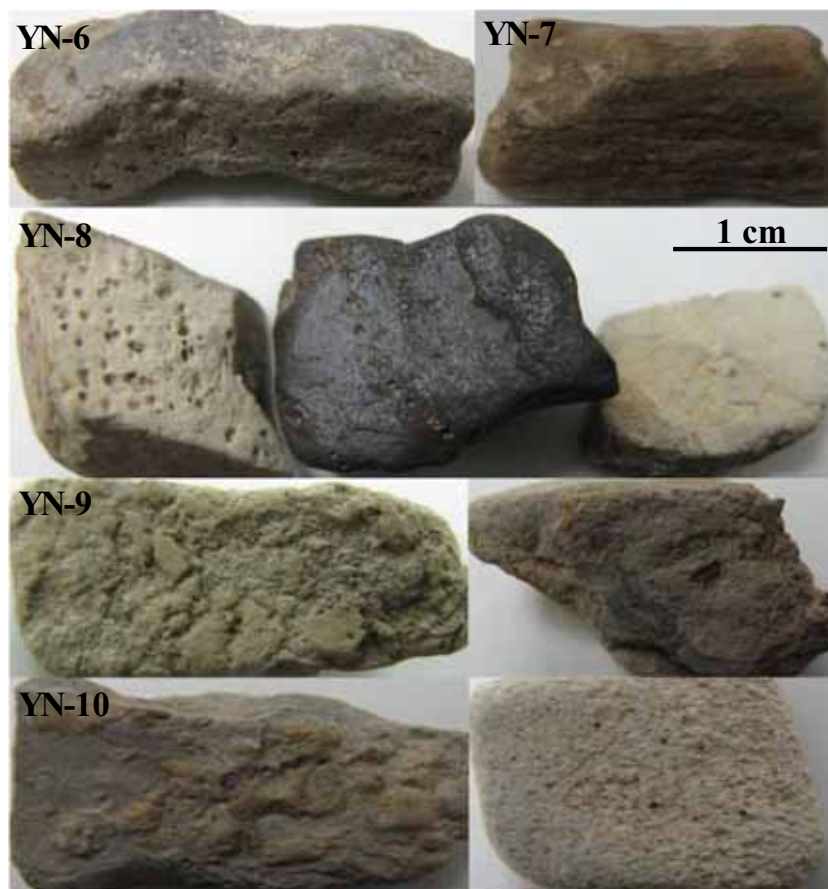


Figure 2. The configuration of gravels in unit 10–70 cm.

distribution parameters (mean grain size, standard deviation, skewness and kurtosis) are very helpful to distinguish different sedimentary environments (Liu *et al.* 2016). We calculated the mean grain size (M_z), standard deviation (σ), skewness (Sk) and kurtosis (K_g) for the subsamples of the sediment profile YN using the method proposed by Blott and Pye (2001), and analyzed compositional characteristics of clay ($< 2 \mu\text{m}$), silt ($2\text{--}63 \mu\text{m}$) and sand ($>63 \mu\text{m}$) contents in YN. The grain size distribution parameters of the middle unit are distinct from the upper and lower unit (figures 3 and 4).

The mean grain size and sorting coefficient of the middle unit are obviously larger than those of the upper and lower units (figure 3A), indicating more coarse particles and poorer sorting. The diameter of till sediment varies significantly, and thus the sorting is very poor (Niekus *et al.* 2016; Van Dijk 2016). In addition, the ternary diagrams of clay, silt and sand compositions (figure 3B) showed that the middle unit ($<2 \text{ mm}$ component) is mainly composed of sand, while the upper and lower units contain more silt.

The scatter diagram of grain size distribution parameters (figure 4) also indicates that the middle unit is significantly different from the upper and lower units. The middle unit is coarse, poorly sorted and more positively skewed, characteristic of glacial till (in general, a well graded, non-sorted mixture of clay, sand, gravel and boulders carried and directly deposited by a glacier without re-sedimentation by other agents) (Landim and Frakes 1968; Niekus *et al.* 2016; Van Dijk 2016).

4.3 Origin of organic matter

The amount and type of organic matter in the lacustrine or ocean sediment encode their depositional palaeoenvironment and palaeoclimate (Meyers 1994; Kołaczek *et al.* 2015; Mirosław-Grabowska *et al.* 2015). C/N ratios and $\delta^{13}\text{C}$ values of organic matter in sediments could preserve palaeoenvironmental information for multi-million years, and have widely been used to identify organic matter sources (Choudhary *et al.* 2009).

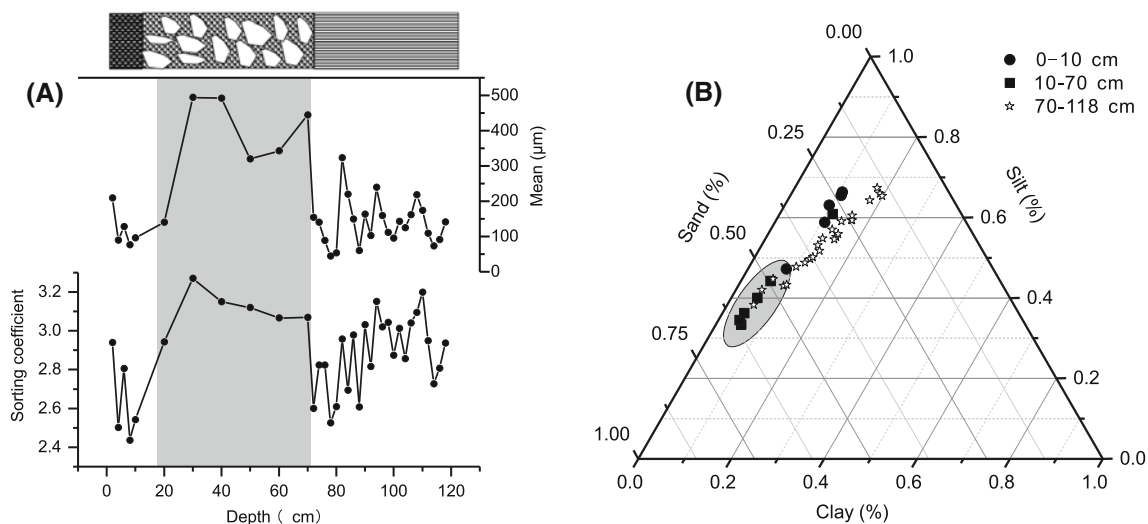


Figure 3. (A) The variation profiles of mean grain size and the sorting coefficient in the palaeo-notch sediment YN, and lithological characteristics of YN. (B) The ternary diagrams of clay, silt and sand compositions in the palaeo-notch sediment YN.

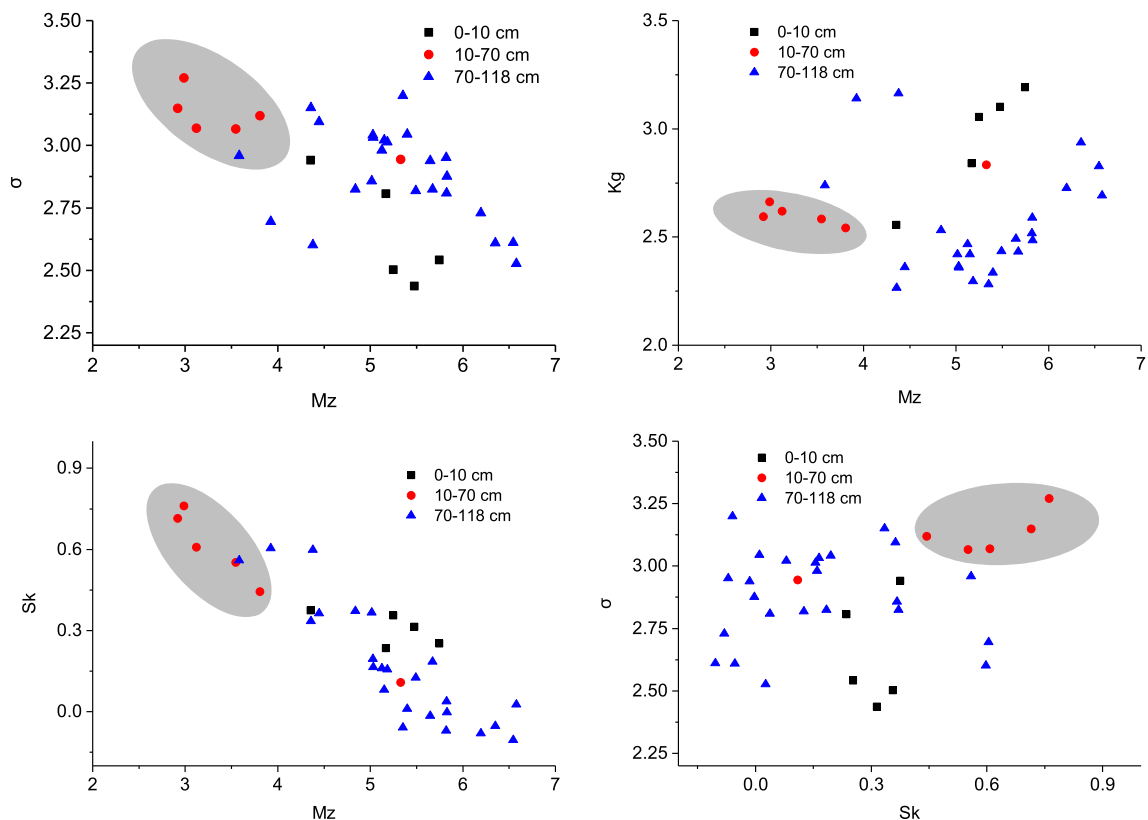


Figure 4. Cross plot of grain size distribution parameters (M_z , σ , S_k and K_g) of the palaeo-notch sediment YN in the upper unit (0–10 cm), middle unit (10–70 cm) and lower unit (70–118 cm), respectively. The shaded area marks the grain size distribution parameters in the middle unit.

The C/N ratios of the middle unit vary significantly from 19 to 55 (figure 5), indicating a complex origin of organic matter. In order to better determine the organic matter sources, C/N ratios and $\delta^{13}\text{C}$ values of three different units in YN, four kinds of common tundra plants and local coal

samples are plotted in figure 5. Half of the samples (Group 1) in the middle unit fall close to four common tundra plants, while the rest (Group 2) fall between the tundra plants and lacustrine sediments (the lower unit and control lake sediments, Yuan *et al.* 2010). Apparently, the organic matters

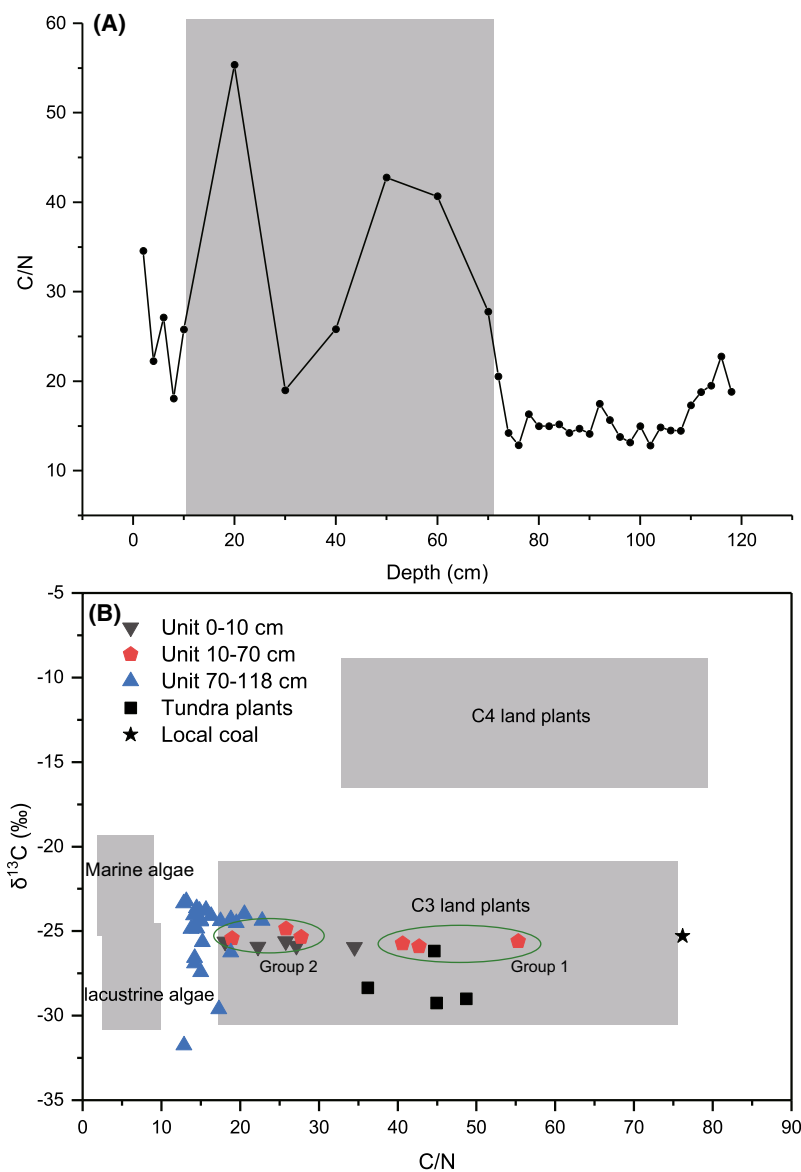


Figure 5. **(A)** Variation profiles of C/N ratios in the palaeo-notch sediment YN. The shaded area marks the C/N ratios in the middle unit (10–70 cm). **(B)** Cross plot of C/N ratios and organic $\delta^{13}\text{C}$ values. The organic $\delta^{13}\text{C}$ values and C/N ratios of organic matter in unit 0–10 cm, 10–70 cm, 70–118 cm, C3 and C4 land plants, marine algae, lacustrine algae, four common tundra plants, and local coal samples are shown in the plot (modified from Meyers 1994 and Yuan *et al.* 2010).

of Group 1 are mainly derived from local tundra plants, and the organic matters of Group 2 are likely influenced by both local tundra plants and lacustrine sediments (figure 5). Therefore, the organic matter of the middle unit is derived from multiple sources, and glacier activity provides a good explanation for the complex origin. During glacier advance, glaciers could erode land surface and bring tundra plants along with the glacial till. When the glacial front reached the sampling site, the surface sediment in the palaeo-notch was likely erased by the glaciers and mixed with the glacial till.

The lithological and grain size characteristics, the C/N ratios, and the $\delta^{13}\text{C}$ values of organic matter of the middle unit all indicate that the middle unit is a glacial till diamicton caused by glacier advance.

4.4 Chronological analysis and palaeoclimatic implications

The chronology of the upper unit determined by excess ^{210}Pb indicated that this unit was deposited in the past 100 yrs, while lower unit was deposited

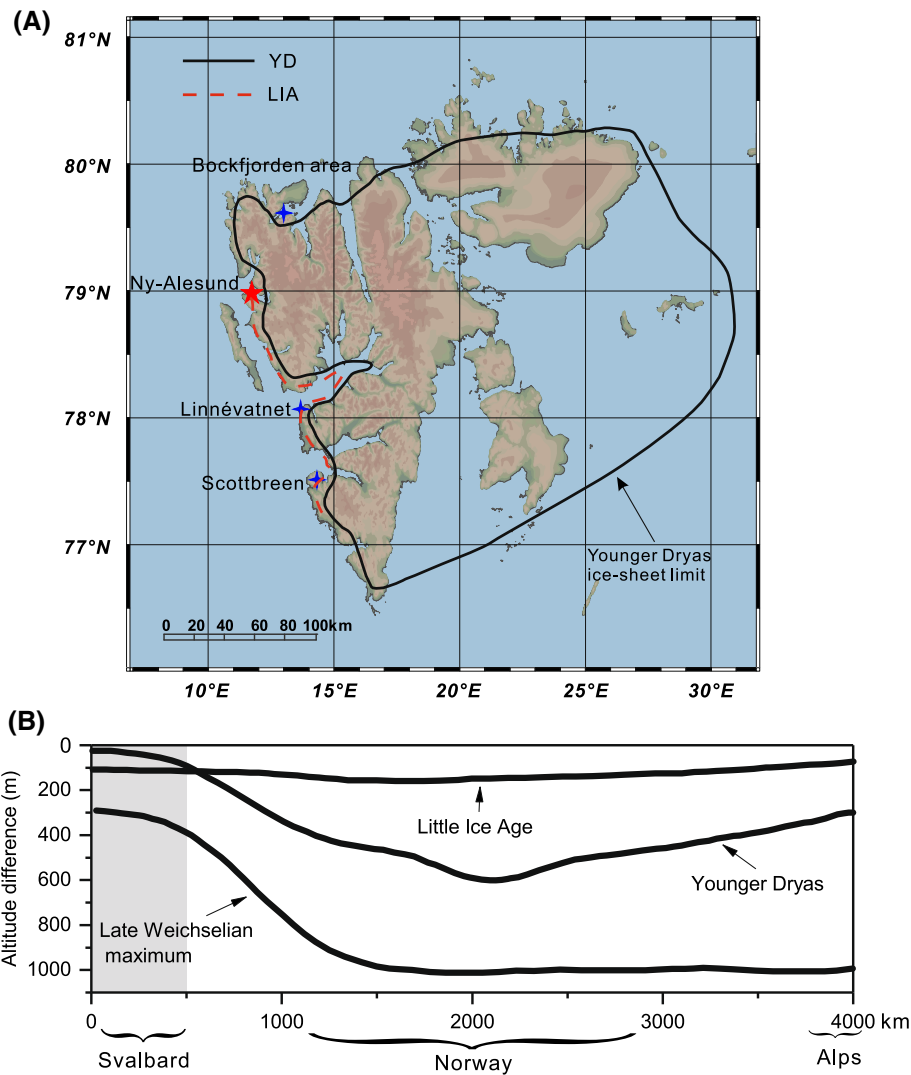


Figure 6. (A) The approximate limit of the Younger Dryas ice sheet on Svalbard (Black line, modified from Svendsen *et al.* 2004 and Mangerud and Landvik 2007). The errors rarely exceeded 30 km along the west coast, while the east coast is more generalized here and errors may exceed 100 km. The red dashed line is the possible limit of the LIA ice sheet on western Spitsbergen. Blue stars mark the location that glaciers during the LIA is more extensive than that during the YD, while the red star marks our sampling site. (B) Estimation of how much lower the ELA was during the LIA, YD and Late Weichselian maximum relative to the present-day ELA (modified from Svendsen *et al.* 2004 and Mangerud and Landvik 2007). The shaded area marks the ELA difference in Svalbard.

from 2219 to 9400 yr BP. Thus, the middle unit was deposited between 2219 yr BP and AD 1900. According to the morphology, origin of organic matter, lithological and grain size characteristics above, the sediments in the middle unit are very likely the glacial till caused by glacier advance. The study area is located near the coastline of the first terrace, far away from the present-day frontiers of ice sheet, and thus only very large and extensive glaciers could reach the sampling site. Because the diamicton was deposited between 2219 yr BP and AD 1900, and large extensive glaciers only happened during the LIA (Salvigsen and Høgvard 2006; Mangerud and Landvik 2007; Røthe *et al.*

2015; Grabiec *et al.* 2018), it is reasonable to assume that the diamicton in the middle unit was deposited during the LIA. In addition, a recent study (Kar *et al.* 2018) also found till sediments caused by glacial activity in the top part of the trench except the topmost humus rich part near the coast of Ny-Alesund, which is consistent with the till sediments recorded in our study.

As the sampling site of YN is located near the coast of Ny-Alesund, the ice margin of the glaciers during the LIA was likely beyond the sampling site, as judging from the thickness of the middle unit, and probably reached up to Kongsfjorden. According to the oceanic investigation in Kongsfjorden, there

exists a long gravel belt parallel to the coast, a large number of gravels are distributed beneath the thin sediment, and it is difficult to collect sediment cores longer than 40 cm therein. This could be the direct evidence for glacial till in Kongsfjorden. However, we did not collect the gravel samples there due to the difficulty in sampling. More future investigations about the glacial till in the ocean are needed to study the glacier activities in Svalbard.

Based on the analysis above, the sediment profile YN has experienced three phases of deposition. The lower unit was accumulated constantly from 9400 to 2219 yr BP (Yang *et al.* 2019). The middle unit is the till-like diamicton caused by glacier advance. The equilibrium line altitude (ELA) of Karlbreen indicated that the LIA period on Svalbard lasted from 450 yr BP to the start of the 20th century (Røthe *et al.* 2015). Therefore, there exists an 1800-yr-long sediment hiatus from 2219 yr BP to AD 1500. The glaciers during the LIA likely removed part of the pre-existing sediments, caused the sediment hiatus between 2219 yr BP and LIA, and led to the formation of the diamicton in the middle unit. After AD 1900, the climate became warm, the LIA ended, and the palaeo-notch began to receive deposit again.

The evidence for more extensive glaciers in western Spitsbergen during the LIA than during the YD were only found in Scottbreen (Mangerud and Landvik 2007), Linnévatnet (Svendsen and Mangerud 1997) and Bockfjorden area (Salvigsen and Høgvard 2006) (figure 6A). This study indicates that the ice margin during the LIA reached the sampling site. However, according to the approximate limit of the YD ice sheet on Svalbard (Svendsen *et al.* 2004; Mangerud and Landvik 2007) (figure 6A), the ice margin did not reach the sampling site during YD. In addition, the ELA of glaciers in western Svalbard during the LIA is significantly lower than that during the YD (Svendsen *et al.* 2004; Mangerud and Landvik 2007) (figure 6B). Therefore, this study may provide a new evidence for more extensive glaciers in Ny-Alesund during the LIA than during the YD, and this is likely related to starvation of precipitation on western Spitsbergen during the YD (Mangerud and Landvik 2007).

In figure 6(A), we also compiled these results together and proposed the approximate limit of the LIA ice sheet in western Spitsbergen. Of course, more relevant research about the LIA ice sheet extent in western Spitsbergen are needed to improve the accuracy of this line.

5. Conclusions

A well-preserved palaeo-notch sediment profile YN in Ny-Alesund was studied which is divided into three units: the upper unit, middle unit and lower unit. The middle unit is a till-like diamicton, it contains many gravels, and it lacks regular lamination. According to the morphological analysis, origin of organic matter, chronological analysis, lithological and grain size characteristics, the sediment in the middle unit is likely the glacial till caused by glacier advance during the LIA. This indicates that the glaciers reached the sampling site during the LIA. Considering the finding that the ice margin of the YD ice sheet on Svalbard did not reach the sampling position during YD, this study may provide a new evidence for more extensive glaciers during the LIA than during the YD in western Spitsbergen.

Acknowledgements

The research was supported by Chinese Polar Environment Comprehensive Investigation & Assessment Programmes (CHINARE2017-02-01, CHINARE2017-04-04). Samples were provided by the Polar Sediment Repository of Polar Research Institute of China (PRIC). Samples information and data were issued by the Resource-sharing Platform of Polar Samples (<http://birds.chinare.org.cn>) maintained by Polar Research Institute of China (PRIC) and Chinese National Arctic & Antarctic Data Center (CN-NADC). We thank the Chinese Arctic and Antarctic Administration and PRIC for logistical support in field.

References

- Ali D O, Spencer A M, Fairchild I J, Chew K J, Anderton R, Levell B K, Hambrey M J, Dove D and Le Heron D P 2017 Indicators of relative completeness of the glacial record of the Port Askaig Formation, Garvellach Islands, Scotland; *Precamb. Res.*, <https://doi.org/10.1016/j.precamres.2017.12.005>.
- Alonso-Muruaga P J, Limarino C O, Spalletti L A and Piñol F C 2018 Depositional settings and evolution of a fjord system during the carboniferous glaciation in Northwest Argentina; *Sedim. Geol.* **369** 28–45.
- Arppe L, Kurki E, Wooller M J, Luoto T P, Zajaczkowski M and Ojala A E 2017 A 5500-year oxygen isotope record of high arctic environmental change from southern Spitsbergen; *The Holocene* **27** 1948–1962.

- Assine M L, de Santa Ana H, Veroslavsky G and Vesely F F 2018 Exhumed subglacial landscape in Uruguay: Erosional landforms, depositional environments, and paleo-ice flow in the context of the late Paleozoic Gondwanan glaciation; *Sedim. Geol.* **369** 1–12.
- Bakke J and Paasche Ø 2011 *Sediment core and glacial environment reconstruction, Encyclopedia of Snow, Ice and Glaciers*; Springer, pp. 979–984.
- Blott S J and Pye K 2001 GRADISTAT: A grain size distribution and statistics package for the analysis of unconsolidated sediments; *Earth Surf. Proc. Land.* **26** 1237–1248.
- Chen A, Tian M, Zhao Z, Qian F and Yao H 2014 Macroscopic and microscopic evidence of Quaternary glacial features and ESR dating in the Daweishan Mountain area, Hunan, eastern China; *Quat. Int.* **333** 62–68.
- Choudhary P, Routh J and Chakrapani G J 2009 An environmental record of changes in sedimentary organic matter from Lake Sattal in Kumaun Himalayas, India; *Sci. Total Environ.* **407** 2783–2795.
- Evans D, Phillips E, Hiemstra J and Auton C 2006 Subglacial till: Formation, sedimentary characteristics and classification; *Earth Sci. Rev.* **78** 115–176.
- Farnsworth W R, Ingólfsson Ó, Noormets R, Allaart L, Alexanderson H, Henriksen M and Schomacker A 2017 Dynamic Holocene glacial history of St. Jonsfjorden, Svalbard; *Boreas* **46** 585–603.
- Forman S L, Mann D H and Miller G H 1987 Late Weichselian and Holocene relative sea-level history of Brøggerhalvøya, Spitsbergen; *Quat. Res.* **27** 41–50.
- Grabiec M, Ignatiuk D, Jania J, Moskalik M, Głowacki P, Błaszczyk M, Budzik T and Walczowski W 2018 Coast formation in an Arctic area due to glacier surge and retreat: The Hornbreen–Hambergbreen case from Spistbergen; *Earth Surf. Proc. Land.* **43** 387–400.
- Gregory A, Balascio N L, D’Andrea W J, Bakke J, Bradley R S and Perren B 2017 Holocene glacier activity reconstructed from proglacial lake Gjøvatnet on Amsterdamøya, NW Svalbard; *Quat. Sci. Rev.* **183** 188–203.
- Guilizzoni P, Marchetto A, Lami A, Brauer A, Vigliotti L, Musazzi S, Langone L, Manca M, Lucchini F, Calanchi N, Dinelli E and Mordenti A 2006 Records of environmental and climatic changes during the late Holocene from Svalbard: Palaeolimnology of Kongressvatnet; *J. Paleolimnol.* **36** 325–351.
- Henriksen M, Alexanderson H, Landvik J Y, Linge H and Peterson G 2014 Dynamics and retreat of the Late Weichselian Kongsfjorden ice stream, NW Svalbard; *Quat. Sci. Rev.* **92** 235–245.
- Hormes A, Gjermundsen E F and Rasmussen T L 2013 From mountain top to the deep sea–deglaciation in 4D of the northwestern Barents Sea ice sheet; *Quat. Sci. Rev.* **75** 78–99.
- Hughes A L, Gyllencreutz R, Lohne Ø S, Mangerud J and Svendsen J I 2016 The last Eurasian ice sheets – a chronological database and time-slice reconstruction, DATED-1; *Boreas* **45** 1–45.
- Kar R, Mazumder A, Mishra K, Patil S K, Ravindra R, Ranhotra P S, Govil P, Bajpai R and Singh K 2018 Climatic history of Ny-Alesund region, Svalbard, over the last 19,000 yr: Insights from quartz grain microtexture and magnetic susceptibility; *Polar Sci.* **18** 189–196.
- Kolaczek P, Mirosław-Grabowska J, Karpińska-Kolaczek M and Stachowicz-Rybka R 2015 Regional and local changes inferred from lacustrine organic matter deposited between the Late Glacial and mid-Holocene in the Skaliska Basin (north-eastern Poland); *Quat. Int.* **388** 51–63.
- Landim P M and Frakes L A 1968 Distinction between tills and other diamictons based on textural characteristics; *J. Sedim. Res.* **38** 1213–1223.
- Landvik J Y, Alexanderson H, Henriksen M and Ingólfsson Ó 2014 Landscape imprints of changing glacial regimes during ice-sheet build-up and decay: A conceptual model from Svalbard; *Quat. Sci. Rev.* **92** 258–268.
- Liu X, Vandenberghe J, An Z, Li Y, Jin Z, Dong J and Sun Y 2016 Grain size of Lake Qinghai sediments: Implications for riverine input and Holocene monsoon variability; *Palaeogeogr. Palaeoclimatol. Palaeoecol.* **449** 41–51.
- Mangerud J and Landvik J Y 2007 Younger Dryas cirque glaciers in western Spitsbergen: Smaller than during the Little Ice Age; *Boreas* **36** 278–285.
- Martín-Moreno R, Allende Álvarez F and Hagen J O 2017 ‘Little Ice Age’ glacier extent and subsequent retreat in Svalbard archipelago; *The Holocene* **27** 1379–1390.
- McClenaghan M B, Paulen R C and Oviatt N M 2018 Geometry of indicator mineral and till geochemistry dispersal fans from the Pine Point Mississippi Valley-type Pb–Zn district, Northwest Territories, Canada; *J. Geochem. Explor.* **190** 69–86.
- Meyers P A 1994 Preservation of elemental and isotopic source identification of sedimentary organic matter; *Chem. Geol.* **114** 289–302.
- Miccadei E, Piacentini T and Berti C 2016 Geomorphological features of the Kongsfjorden area: Ny-Ålesund, Blomstrandøya (NW Svalbard, Norway); *Rendiconti Lincei* **27** 217–228.
- Mirosław-Grabowska J, Niska M and Kupryjanowicz M 2015 Reaction of lake environment on the climatic cooling – Transition from the Eemian Interglacial to Early Vistulian on the basis of Solniki palaeolake sediments (NE Poland); *Quat. Int.* **386** 158–170.
- Mottin T E, Vesely F F, de Lima Rodrigues M C N, Kipper F and de Souza P A 2018 The paths and timing of late Paleozoic ice revisited: New stratigraphic and paleo-ice flow interpretations from a glacial succession in the upper Itararé Group (Paraná Basin, Brazil) *Palaeogeogr. Palaeoclimatol. Palaeoecol.* **490** 488–504.
- Niekus M T, Van Balen R, Bongers J, Bosch J, Brinkhuizen D, Huisman H, Jelsma J, Johansen L, Kasse C and Kluiwing S 2016 News from the north: A late Middle Palaeolithic site rich in handaxes on the Drenthe–Frisian till plateau near Assen, the Netherlands. First results of a trial excavation; *Quat. Int.* **411** 284–304.
- Oerlemans J 2005 Extracting a climate signal from 169 glacier records; *Science* **308** 675–677.
- Osuch M and Wawrzyniak T 2017 Inter- and intra-annual changes in air temperature and precipitation in western Spitsbergen; *Int. J. Climatol.* **37** 3082–3097.
- Røthe T O, Bakke J, Vasskog K, Gjerde M, D’Andrea W J and Bradley R S 2015 Arctic Holocene glacier fluctuations reconstructed from lake sediments at Mitrhalvøya, Spitsbergen; *Quat. Sci. Rev.* **109** 111–125.
- Reusche M, Winsor K, Carlson A E, Marcott S A, Rood D H, Novak A, Roof S, Retelle M, Werner A and Caffee M 2014

- 10 Be surface exposure ages on the late-Pleistocene and Holocene history of Linnébreen on Svalbard; *Quat. Sci. Rev.* **89** 5–12.
- Ruiz-Fernández A C, Hillaire-Marcel C, Páez-Osuna F, Ghaleb B and Soto-Jiménez M 2003 Historical trends of metal pollution recorded in the sediments of the Culiacan River Estuary, Northwestern Mexico; *Appl. Geochem.* **18** 577–588.
- Salvigsen O and Høgvard K 2006 Glacial history, Holocene shoreline displacement and palaeoclimate based on radiocarbon ages in the area of Bockfjorden, north-western Spitsbergen, Svalbard; *Polar Res.* **25** 15–24.
- Sessford E G, Strzelecki M C and Hormes A 2015 Reconstruction of Holocene patterns of change in a High Arctic coastal landscape, Southern Sassenfjorden, Svalbard; *Geomorphology* **234** 98–107.
- Solomina O N, Bradley R S, Hodgson D A, Ivy-Ochs S, Jomelli V, Mackintosh A N, Nesje A, Owen L A, Wanner H and Wiles G C 2015 Holocene glacier fluctuations; *Quat. Sci. Rev.* **111** 9–34.
- Solomina O N, Bradley R S, Jomelli V, Geirsdottir A, Kaufman D S, Koch J, McKay N P, Masiokas M, Miller G and Nesje A 2016 Glacier fluctuations during the past 2000 years; *Quat. Sci. Rev.* **149** 61–90.
- Sovetov J 2015 Tillites at the base of the Vendian Taseeva Group in the stratotype section (Siberian craton); *Russian Geol. Geophys.* **56** 1522–1530.
- Sun L, Liu X, Yin X, Xie Z and Zhao J 2005 Sediments in palaeo-notches: Potential proxy records for palaeoclimatic changes in Antarctica; *Palaeogeogr. Palaeoclimatol. Palaeoecol.* **218** 175–193.
- Svendsen J I, Briner J P, Mangerud J and Young N E 2015 Early break-up of the Norwegian channel ice stream during the last glacial maximum; *Quat. Sci. Rev.* **107** 231–242.
- Svendsen J I, Gataullin V, Mangerud J and Polyak L 2004 The glacial history of the Barents and Kara Sea region; *Quaternary Glaciations – Extent and Chronology* **1** 369–378.
- Svendsen J I and Mangerud J 1997 Holocene glacial and climatic variations on Spitsbergen, Svalbard; *The Holocene* **7** 45–57.
- Swift D A, Cook S J, Graham D J, Midgley N G, Fallick A, Storrar R, Rodrigo M T and Evans D 2018 Terminal zone glacial sediment transfer at a temperate overdeepened glacier system; *Quat. Sci. Rev.* **180** 111–131.
- Szczuciński W, Zajaczkowski M and Scholten J 2009 Sediment accumulation rates in subpolar fjords—Impact of post-Little Ice Age glaciers retreat, Billefjorden, Svalbard; *Estuarine, Coast. Shelf Sci.* **85** 345–356.
- van der Bilt W G M, Bakke J, Vasskog K, D’Andrea W J, Bradley R S and Ólafsdóttir S 2015 Reconstruction of glacier variability from lake sediments reveals dynamic Holocene climate in Svalbard; *Quat. Sci. Rev.* **126** 201–218.
- Van Dijk N 2016 Experimental investigation to the settling and consolidation of dredged glacial till; uuid:1c0060de-0068f0066a-0064e0024-beae-0069cca0062bf0073e0042.
- Yang Z, Sun L, Zhou X and Wang Y 2018 Mid to late Holocene climate change record in palaeo-notch sediment from London Island, Svalbard; *J. Earth Syst. Sci.* **127** 57.
- Yang Z, Wang J, Yuan L, Cheng W, Wang Y, Xie Z and Sun L 2019 Total photosynthetic biomass record between 9400 and 2200 BP and its link to temperature changes at a High Arctic site near Ny-Ålesund, Svalbard; *Polar Biol.* **42** 991–1003, <https://doi.org/10.1007/s00300-019-02493-5>.
- Yuan L, Sun L, Long N, Xie Z, Wang Y and Liu X 2010 Seabirds colonized Ny-Ålesund, Svalbard, Arctic ~9,400 years ago; *Polar Biol.* **33** 683–691.
- Yuan L, Sun L, Wei G, Long N, Xie Z and Wang Y 2011 9,400 yr BP: The mortality of mollusk shell (*Mya truncata*) at high Arctic is associated with a sudden cooling event; *Environ. Earth Sci.* **63** 1385–1393.

Corresponding editor: SANTANU BANERJEE